The Nonlinear Mechanical Behaviour of Composite Materials Reinforced with Carbon Fiber Weaves

MARIUS MARINEL STANESCU[1]*, DUMITRU BOLCU[2], ION CIUCA[3], SABIN RIZESCU[2], OCTAVIAN TRANTE[3], MIHAI BAYER[4]

[1] University of Craiova, Department of Applied Mathematics, 13 A.I. Cuza, 200396, Craiova, Romania

[2] University of Craiova, Department of Mechanics, 165 Calea Bucureşti, 200620, Craiova, Romania

[3] Politehnica University of Bucharest, Department of Materials Science and Engineering, 313 Splaiul Independenţei, 060032,

[4] Politehnica University of Bucharest, Department of Biotechnical Systems Engineering, 313 Splaiul Independentei, 060042, Bucharest, Romania

This work paper proposes an elastic displacement field for a composite bar made of two constituents (phases). The deformation hypothesis described by this field is built in full respect of all the conditions of compatibility concerning deformation and strain-stress status of any kind. More else, the conditions of continuity concerning the surface separating the two constituents are also fully satisfied. Using this new displacement field we show that the tangent to each and every point of the characteristic curve built for this composite material depends only on the size of external charge (loading) and the longitudinal deformation of the composite bar. Based on these facts we also show that the constitutive equation of this composite material is a non-linear one: in fact it is a concave curve the way that the slope of the tangent to each and every point of the characteristic curve is decreasing as the deformation increases. We have released three sample groups with different arrangements of reinforcing fibers from one group to any other one and we have established the characteristic curve for each and every sample group. Using these curves we have obtained the longitudinal elasticity modulus, the tension at break, the elongation at break as well as the slope and the ordinate at the origin for the tangent to the breaking point of the characteristic curve. The characteristic curves have the shape (allure) suggested by the theoretically obtained results. We have shown that a certain parameter characterizing the non-linear behavior of the composite material is given by the ratio between the longitudinal elasticity modulus and the value of the slope of the tangent to the breaking point of the composite material characteristic curve.

Keywords: composite materials, characteristic curve, elasticity modulus

In composite materials containing fiber or particulate reinforcement the interface separating matrix from inclusion is widely believed to be a dominant influence affecting the overall stiffness and damage tolerance characteristics of the composite. Likewise damage accumulation in a composite often depends on the character of the mechanical response of the interface that, in the case of a weak interface, may precipitate such separation phenomena as brittle or ductile decohesion. In many fiber-reinforced composite systems weak interfaces or desirable since they generally raise the toughness, however, are often at the expense of composite stiffness. Accurate assessment of overall stiffness characteristics of a composite containing fiber weakly bonded to the matrix is therefore extremely important in the attempt to obtain improved composite performance.

Numerous models currently exist to obtain the effective moduli of spherical and cylindrical composite systems which, for linear elastic constituent behavior and coherently bonded interfaces, are reviewed in [1-4]. Because the standard material models require for their implementation the solution to a solitary inclusion-interface-matrix system the problem of obtaining effective material properties for a composite is, to a large extend, dependent on the availability of the elastic field solutions to the solitary problem. For the case of a unidirectional fiber-reinforced composite which can reasonably be regarded as having effective transverse isotropic and homogeneous material properties this amounts to the solution of the solitary problem under a variety of loading conditions.

Employing the method of cells [3-5] have been obtained effective properties of fiber-reinforced materials which allow for only shear interface discontinuities while [6] utilizes the same method and allows for linear shear and normal interface force-separation behaviour. The interface was characterized by a linear relation between interfacial traction and interfacial displacement jump so that phenomenon of cavity formation by interfacial decohesion was not accounted for. In [7] is represented a natural extension of existing model in which a more realistic nonlinear interface separation mechanism is considered in the problem of effective transverse bulk response of a composite containing random distribution of unidirectional linear elastic fibers embedded in a linear elastic matrix in dilute and nondilute concentration. In the solitary fiber problem interface characterization assumed the form of a nonlinear force-separation law which couples the normal component of displacement jump to the normal component of interface traction and which requires a characteristic length for its prescription. Interaction effects due to finite fiber volume concentration, along with the phenomenon of brittle decohesion arising in the solitary fiber problem from the bifurcation of equilibrium separation at the fiber matrix interface, are shown to precipitate instability in the composite.

Nonlinear viscoelastic behavior has been observed in laboratory tests of polymer matrix composites [8-10]. Elastic approaches cannot accurately predict residual stress and strain fields since material properties and strengths of polymeric matrix composite are strongly time dependent [11-12]. In composite structural design, time-

* *email: mamas1967@gmail.com*

dependent effects of polymer matrix composite materials must be considered in order to ensure realistic analysis and the environmental durability over the entire life span of composite structures.

Interlaminar stresses near free edges are mainly responsible for delamination failures. Numerous studies have been undertaken to investigate interlaminar stresses and failures of laminated composites. In [11] is studied the interlaminar tensile strength under static and fatigue loads including the temperature and moisture effects. In [13] is studied the effect of geometric nonlinearities on free-edge stress fields. In [14] is investigated the response and failure for dropped-ply laminates tested in flat-end compression, and [15] have shown that the times for delamination onset occurrences in composites can predicted probabilistically. Their analysis includes stochastic processes due to combined random loads and random delamination failure stresses as well as random anisotropic viscoelastic material properties.

A finite element formulation for analyzing interlaminar stress fields in nonlinear anisotropic viscoelastic laminated composites, including a hydrothermal formulation, is presented in [16, 23-28, 30]. The results indicate a strong sensitivity to the nonlinearities of the viscoelastic constitutive relations.

For composite materials like boron-epoxy resin or graphite – epoxy resin a non-linear behaviour appears due to the material matrix that affects mainly the shear modulus [17, 22]. Similar results have been obtained in [18,19, 29]. In [20, 21] some studies have been made on the non-linear behaviour of the composite plates having epoxy or phenolic based matrix and being randomly reinforced.

Theoretically-obtained results

Let's consider a displacement status having the following form:

$$\begin{aligned} &w_1(x_1,x_2,x_3) = (k + ax_3)x_1 + h(x_2,x_3),\\ &w_2(x_1,x_2,x_3) = u(x_3)\cdot\sin(\alpha\, x_2),\\ &w_3(x_1,x_2,x_3) = Ax_1^2 + Bx_1 +\\ &+ Cx_3^2 + Dx_3 + v(x_3)\cos(\alpha\, x_2). \end{aligned} \tag{1}$$

The components of the deformation tensor will be calculated using the following relations:

$$\varepsilon_{ij} = \frac{1}{2}\left(\frac{\partial w_i}{\partial x_j} + \frac{\partial w_j}{\partial x_i}\right). \tag{2}$$

We obtain:

$$\begin{aligned} &\varepsilon_{11} = k + ax_3,\\ &\varepsilon_{22} = \alpha\, u(x_3)\cos(\alpha\, x_2),\\ &\varepsilon_{33} = 2Cx_3 + D + v'(x_3)\cos(\alpha\, x_2),\\ &\varepsilon_{12} = \frac{1}{2}\frac{\partial h}{\partial x_2},\\ &\varepsilon_{13} = \frac{1}{2}\left(ax_1 + \frac{\partial h}{\partial x_3} + 2Ax_1 + B\right),\\ &\varepsilon_{23} = \frac{1}{2}(u'(x_3) - \alpha\, v(x_3))\sin(\alpha\, x_2). \end{aligned} \tag{3}$$

The Saint-Venant are fulfilled and that can be verified immediately:

$$\frac{\partial^2\varepsilon_{ij}}{\partial x_k\partial x_l} + \frac{\partial^2\varepsilon_{kl}}{\partial x_i\partial x_j} = \frac{\partial^2\varepsilon_{ik}}{\partial x_j\partial x_l} + \frac{\partial^2\varepsilon_{jl}}{\partial x_i\partial x_k}. \tag{4}$$

The strain-stress status is given by Hooke equation. We obtain:

$$\begin{aligned} &\sigma_{11} = c_{11}(k + ax_3) + c_{12}\alpha u(x_3)\cos(\alpha x_2) +\\ &+ c_{13}(2Cx_3 + D + v'(x_3)\cos(\alpha x_2)),\\ &\sigma_{22} = c_{12}(k + ax_3) + c_{22}\alpha u(x_3)\cos(\alpha x_2) +\\ &+ c_{23}(2Cx_3 + D + v'(x_3)\cos(\alpha x_2)),\\ &\sigma_{33} = c_{13}(k + ax_3) + c_{23}\alpha u(x_3)\cos(\alpha x_2) +\\ &+ c_{33}(2Cx_3 + D + v'(x_3)\cos(\alpha x_2)),\\ &\sigma_{12} = c_{66}\frac{\partial h}{\partial x_2},\\ &\sigma_{13} = c_{55}\left(ax_1 + \frac{\partial h}{\partial x_3} + 2Ax_1 + B\right),\\ &\sigma_{23} = c_{44}(u'(x_3) - \alpha\, v(x_3))\sin(\alpha\, x_2), \end{aligned} \tag{5}$$

where c_{11}, c_{22}, c_{33},c_{12},c_{13},c_{23},c_{44},c_{55},c_{66}, have constant values and depend only on the nature of the material.

The components of the strain-stress tensor have to satisfy the Cauchy equilibrium equations:

$$\sum_{j=1}^{3}\frac{\partial\sigma_{ij}}{\partial x_j} = 0,\ i = 1,\ 2,\ 3. \tag{6}$$

The following relations are obtained:

$$\begin{aligned} &c_{66}\frac{\partial^2 h}{\partial x_2^2} + c_{55}\frac{\partial^2 \bar{h}}{\partial x_3^2} = 0,\\ &c_{44}u''(x_3) - \alpha^2 c_{22}u(x_3) -\\ &-\alpha(c_{23} + c_{44})\cdot v'(x_3) = 0,\\ &c_{33}v''(x_3) - \alpha^2 c_{44}v(x_3) + \alpha(c_{23} + c_{44})\cdot u'(x_3) +\\ &+ (c_{55} + c_{13})a + 2c_{55}A + 2c_{33}C = 0. \end{aligned} \tag{7}$$

In the case of homogenous materials:

$$\begin{aligned} &c_{11} = c_{22} = c_{33} = \frac{E(1-\upsilon)}{(1-2\upsilon)(1+\upsilon)},\\ &c_{12} = c_{13} = c_{23} = \frac{E\upsilon}{(1-2\upsilon)(1+\upsilon)},\\ &c_{44} = c_{55} = c_{66} = \frac{E}{2(1+\upsilon)}, \end{aligned} \tag{8}$$

where E is the Young modulus and υ is the Poisson ratio.

In the case of homogenous materials the functions $u(x_3)$ and $v(x_3)$ take the following form:

$$\begin{aligned} &u(x_3) = (c_1x_3 + c_2)e^{\alpha x_3} + (c_3x_3 + c_4)e^{-\alpha x_3} + k_1,\\ &v(x_3) = (c_5x_3 + c_6)e^{\alpha x_3} + (c_7x_3 + c_8)e^{-\alpha x_3} + k_2, \end{aligned} \tag{9}$$

where the constants resulting from integration, c_1,....c_8, will be determined from the boundary conditions the strain-stress field has to fulfill on the free faces of the material.

Let's consider a composite bar made of two homogenous constituents. Its right transverse section is considered as being a rectangular one (fig. 1) and Ox_1, x_2, is the separation plan between the two constituents.

Under the action of certain external forces each constituent deformes itself the way that the displacement status is given by relations like (1).

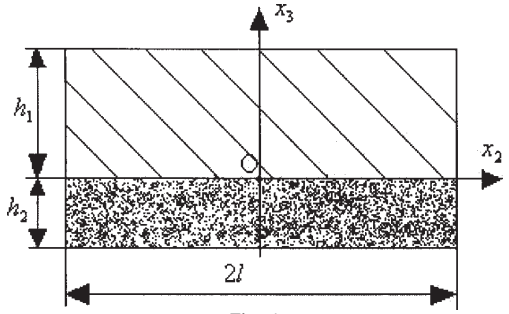

Fig. 1.

Lets's consider:

$\varepsilon_{ij}^{(1)}$, $i, j = \overline{1,3}$, the components of the deformation tensor for the constituent No. 1;

$\varepsilon_{ij}^{(2)}$, $i, j = \overline{1,3}$, the components of the deformation tensor for the constituent No. 2;

$\sigma_{ij}^{(1)}$, $i, j = \overline{1,3}$, the components of the deformation tensor for the constituent No. 1;

$\sigma_{ij}^{(2)}$, $i, j = \overline{1,3}$, the components of the deformation tensor for the constituent No. 2.

On the separation surface between the two constituents the following conditions of continuity must be fulfilled:

-for the strain-stress status

$$\begin{aligned} \sigma_{13}^{(1)}\big|_{x_3=0} &= \sigma_{13}^{(2)}\big|_{x_3=0}; \\ \sigma_{23}^{(1)}\big|_{x_3=0} &= \sigma_{23}^{(2)}\big|_{x_3=0}; \\ \sigma_{33}^{(1)}\big|_{x_3=0} &= \sigma_{33}^{(2)}\big|_{x_3=0}; \end{aligned} \tag{10}$$

-for the deformation status

$$\begin{aligned} \varepsilon_{11}^{(1)}\big|_{x_3=0} &= \varepsilon_{11}^{(2)}\big|_{x_3=0}; \\ \varepsilon_{22}^{(1)}\big|_{x_3=0} &= \varepsilon_{22}^{(2)}\big|_{x_3=0}; \\ \varepsilon_{12}^{(1)}\big|_{x_3=0} &= \varepsilon_{12}^{(2)}\big|_{x_3=0}. \end{aligned} \tag{11}$$

On the free faces of the composite bar the following conditions must be fulfilled:

-on the upside surface:

$$\begin{aligned} \sigma_{13}^{(1)}\big|_{x_3=h_1} &= 0; \\ \sigma_{23}^{(1)}\big|_{x_3=h_1} &= 0; \\ \sigma_{33}^{(1)}\big|_{x_3=h_1} &= 0; \end{aligned} \tag{12}$$

-on the downside surface

$$\begin{aligned} \sigma_{13}^{(2)}\big|_{x_3=-h_2} &= 0; \\ \sigma_{23}^{(2)}\big|_{x_3=-h_2} &= 0; \\ \sigma_{33}^{(2)}\big|_{x_3=-h_2} &= 0; \end{aligned} \tag{13}$$

-on the lateral surfaces

$$\begin{aligned} \sigma_{12}^{(1)}\big|_{x_2=\pm l} &= \sigma_{12}^{(2)}\big|_{x_2=\pm l} = 0; \\ \sigma_{22}^{(1)}\big|_{x_2=\pm l} &= \sigma_{22}^{(2)}\big|_{x_2=\pm l} = 0; \\ \sigma_{23}^{(1)}\big|_{x_2=\pm l} &= \sigma_{23}^{(2)}\big|_{x_2=\pm l} = 0. \end{aligned} \tag{14}$$

We shall define the medium average longitudinal in the right transverse section of the composite bar:

$$\varepsilon = \frac{1}{S}\iint_S \varepsilon_{11} dS, \tag{15}$$

where S is the aria of the right transverse section of the bar.

The same way we define the normal medium average stress (effort) in the right transverse section of the bar:

$$\sigma = \frac{1}{S}\iint_S \sigma_{11} dS. \tag{16}$$

In case that the relations (10 – 14) are fulfilled, we obtain:

$$\begin{cases} \varepsilon = k + \left(\sum_{i=1}^{2} \frac{1+\upsilon_i}{2E_i}\cdot \nu_i\right)\beta, & (17) \\ \sigma = \left(\sum_{i=1}^{2} \frac{E_i}{1+\upsilon_i}\cdot \nu_i\right)k + \left(\sum_{i=1}^{2} \frac{1+\upsilon_i}{2(1-\upsilon_i)}\cdot \nu_i\right)\beta, & (18) \end{cases}$$

where:

- k is the longitudinal deformation for $x_3 = 0$;
- β characterizes the continuity of streses(efforts) for $x_3 = 0$;
- E_i, ν_i, are the Young modulus and the Poisson ratio for the „i" (i=1,2) constituent;
- V_i(i=1,2) is the volumetric ratio for the „i" material.

Using the relations (17) and (18) we can obtain a direct relation between the medium average stress (effort) and the medium average deformation like the following one:

$$\sigma = m\varepsilon + n. \tag{19}$$

For extremely low values of external charge (loading), the m parameter coincides with the longitudinal elasticity modulus and decreases as the external charge (loading) increases. Meanwhile n increases as the external charge (loading) increases, starting with the „0" value. So, the relation (19) cannot be accepted as a constitutive equation for the entire composite material. The relation (19) can be accepted as the equation of the right tangent to the point (ε,σ) of the characteristic curve (length). The characteristic curve (length) results from wrapping of all tangents of this kind (fig. 2).

Because both medium average deformation and medium average stress (effort) depend on k and β, it becomes obvious that the longitudinal elasticity modulus could have values contained in some kind of „range". A range of this kind depends on the value of these parameters.

For example, considering the values $k = 0$ and β=0, the corresponding longitudinal elasticity modulus is different from the same modulus obtained for $k \neq 0$ and β=0. In fact, both k and β are different from zero. So, the longitudinal elasticity modulus has to be obtained using experimental methods.

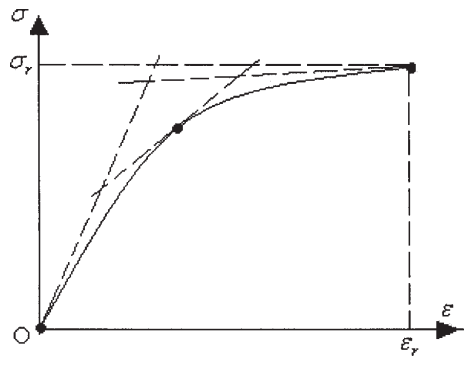

Fig. 2.

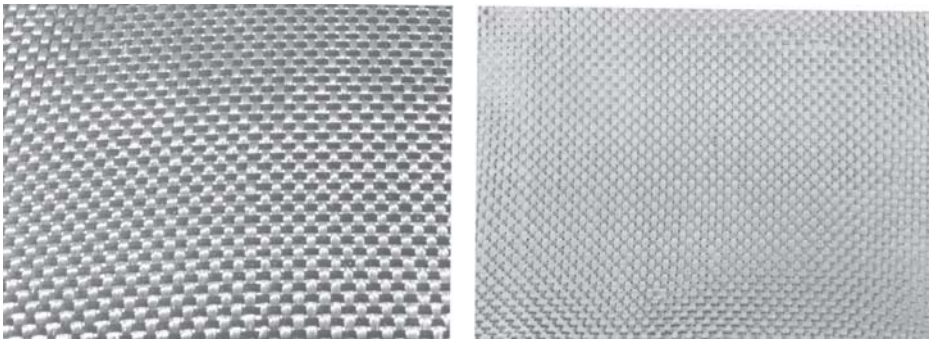

Fig. 3a, b

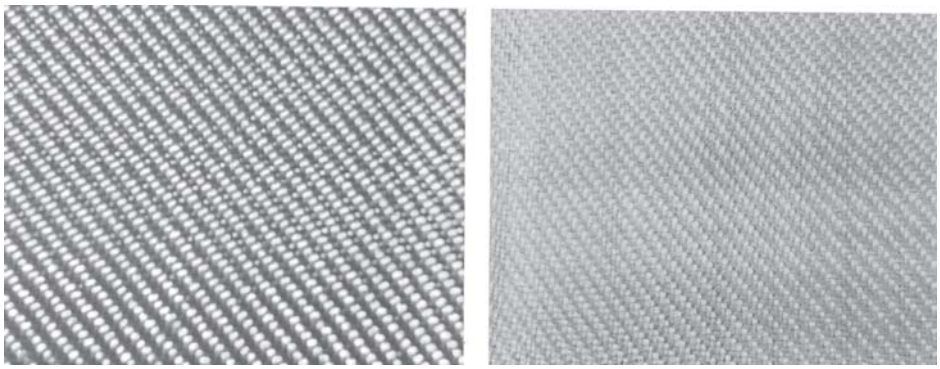

Fig. 4a, b

Experimental results

We have released three sample groups of carbon fiber reinforced composite materials having their matrix made of epoxy resin.

For the first sample group a carbon fiber called „A" type was used. This fiber is presented in the figure 3 (from face 3a, from behind 3b).

For the second sample group a carbon fiber called „B" type was used. This fiber is presented in the figure 4 (from face 4a, from behind 4b).

The third sample group containes samples were reinforced with alternative layers of both „A" and „B" fiber types.

Test-pieces have been released from each and every group of samples. Each and every test-piece has supported a tensile test.

The characteristic curve (length) corresponding to a test-piece having reinforcing of „A" type is presented in the figure 5.

The characteristic curve (length) corresponding to a test-piece having reinforcing of „B" type is presented in the figure 6.

The characteristic curve (length) corresponding to a test-piece having reinforcing of both „A" and „B" types is presented in the figure 7.

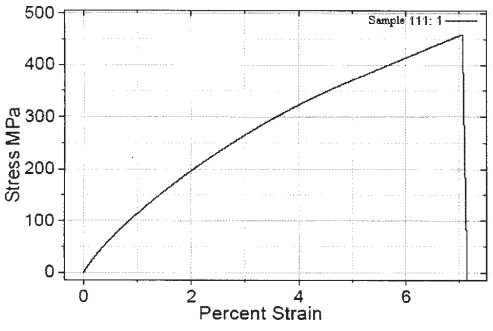

Fig. 5

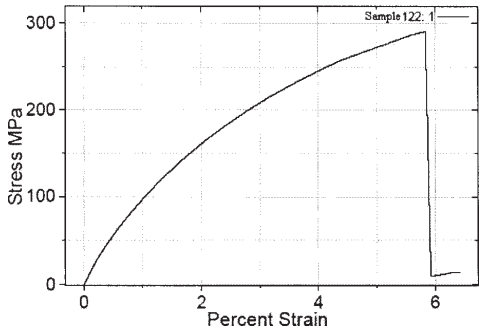

Fig. 6

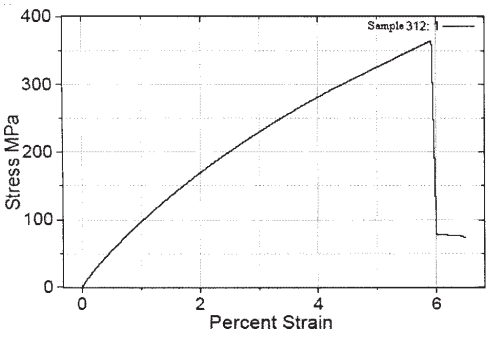

Fig. 7

The thickness, the width and the distance between tanks were measured using a digital slide rule. All the other values were read on the computer screen right after the test was made.

Analyzing all data we can pick up the main mechanical and strength-related characteristics of materials being parts of experiments (tensile strength, tensile-break elongation). These characteristics are presented in the table 1.

The equations of tangents at the beginning points (the origins of the axis system) and at the break points of the characteristic curves were determined.

Using those equations, the longitudinal elasticity modulus, the slope and the ordinate at the origin of the

Table 1

Sample group	Thickness $[mm]$	Width $[mm]$	Distance between tanks $[mm]$	σ_{max} $[MPa]$	σ_{rup} $[MPa]$	ε_{rup} $[\%]$	Energy $[J]$	$\sigma_{0,2}$ $[MPa]$
1	1.27	18.49	20.54	459	459	7	9	368
2	1.24	18.43	20.54	290	290	6	5	257
3	1.07	18.28	20.55	364	364	6	5	344

Table 2

Sample group	Longitudinal elasticity modulus $[MPa]$	Coefficients of the tangent to the break point of the characteristic curve $[MPa]$	
		m	n
1	13432	4572	145
2	12060	2224	162
3	10781	4388	103

Remark: A wide difference between the longitudinal elasticity modulus and the value of m in the break point could be interpreted as a measure of the non-linear behaviour of the composite material

tangent to the break point. All these issues are presented in the table 2.

Conclusions

The theoretical expressions we are proposing for the displacement field were found the way that they are fully satisfying both the compatibility conditions for deformations and stresses (efforts) (Saint Venant and Cauchy).

All the continuity conditions for deformations and stresses (efforts) on the separation surface between constituents as well as for the free surfaces of the material were fulfilled.

The obtained theoretical results are making good predictions on existing non-linearities, as wel as for their limits without (unfortunately) determinining the exact form of the constitutive equations for the composite materials.

The experimental results (the experimental-obtained characteristic curves) confirm the theoretically-obtained results.

The analysis of the characteristic curves confirms the arise of non-linear dependence between the stres and deformation and that way anticipated in the theoretical approach.

The slope of the tangent to each and every point of the characteristic curve is decreasing as the deformation increases and meaning that the second derivative of the function describing the characteristic curve takes only negative values and, as consequence, the curve is a concave one.

We, also, may conclude that, if the charges (loadings) wouldn't be kind of continous, the elasticity modulus would decrease from a loading to a next one. This fact could be explained through the arising plastic phenomena even at the beginning of a loading proces. These plastic phenomena are possible because the strain-stres status corresponding .

to reinforcing fibers are significantly different from those corresponding to matrix and, so, those which constiuents tend to deform themselves differently and the deformation tensor will be not a linear one (the displacement field will be described by non-linear functions).

Some other potential reasons for the non-linear behaviour could be:

- the reinforced fibers are not simultaneously put in charge because the fabric is not perfect: it actually might contain some „curved" fibers that are taking the charge after they reach the right form;

- some sliding phenomena on the separation surface between constituents;

- due to the fiber-form of the reinforcing constituent, the volumetric ratio of the reinforcing constituent might differ from one zone to another of the composite material.

References

1. CHRISTENSEN, R.M., LO. K.H., Solutions for the effective shear properties in three phase sphere and cylinder models, Journal of the Mechanics and Physics of Solids, **27**, 1979, p. 315

2.HASKIN, Z., Analysis of composite materials, ASME J. Appl. Mech., **50**, 1983, p. 481

3.ABOUDI, J., Mechanics of composite materials, Elsevier, Amsterdam, 1991

4.NEMAT-NASSER, S., HORI, M., Micromechanics: overall properties of heterogeneous materials, North-Holland, Amsterdam, 1993

5.BENEVISTE, Y., ABOUDI, J., A continuum model for fiber reinforced materials with debonding, International Journal of Solids and Structures, **20**, 1984, p. 935

6.ABOUDI, J., Damage in composite-modeling of imperfect bonding, Composite Science and Technology, **28**, 1987, p. 103-128.

7.LEVY, A.J., The effective dilatational response of fiber-reinforced composites with nonlinear interface, Journal of Applied Mechanics, **63**(2), 1996, p. 357

8. HARPER, B.D., WEISTMAN, Y., On the effects of environmental conditioning on residual stresses in composites laminates, International Journal of Solids and Structures, **21**, 1985, p. 907-926.

9. TUTTLE, M.E., BRISON, H.F., Prediction of the long-term creep compliance of general composite laminates, Experimental Mechanics, **20**(1), 1986, p. 89

10.WALRATH, D.E., Viscoelastic response of a unidirectional composite containing two viscoelastic constituents, Experimental Mechanics, **31**(6), 1986, p. 111

11.HIEL, C.C., SUMICH, M., CHAPPELL, D.P., A curved beam test specimen for determining the interlaminar tensile strength of a laminated composite, Journal of Composite Materials, **25**, 1991, p. 854-868.

12.YI, S., Thermo-viscoelastic analysis of delamination onset and free edge response in epoxy matrix composite laminates, AIAA Journal, **31**(12), 1993, p. 2320

13.GU, Q., REDDY, J.N., Non-linear analysis of free-edge effects in composite laminates subjected to axial loads, International Journal of Non-Linear Mechanics, 276, 1992, p. 27

14.DAVILA, C.G., JOHNSON, E.R., Analysis of delamination initiation in postbuckled dropped-ply laminates, AIAA Journal, **31**, no. 4, 1993, p. 721

15.HILTON, H.H., YI, S., Stochastic viscoelastic delamination onset failure analysis of composite, Journal of Composite Materials, **27**, no. 11, 1993, p. 1097

16.YI, S., HILTON, H.H., AHMAD, M.F., Nonlinear thermo-viscoelastic analysis of interlaminar stresses in laminated composites, Journal of Applied Mechanics, **63**, no. 1, 1996, p. 218

17.ZHOU, J., HE, T., On the analysis of the end-notched flexure specimen for measuring mode, fracture toughness of composite materials, Composite Science and Technology, **50**, no. 2, 1994, p. 209
18.CASCAVAL, C-TIN., ROSU, D., ROSU, L.,Mat. Plast., **36**, no. 1, 2005, p. 76
19.PUSCA, ST., PAUN, M.A., TOMA, C., Mat. Plast., **44**, no. 1, 2007, p. 39
20.BOLCU, D., STĂNESCU, M.M., CIUCA, I., TRANTE, O., MAYER, M., Mat. Plast., **46**, no. 2, 2009, p. 206
21.CIUCA, I., STĂNESCU, M.M., BOLCU, D., MOTOMANCEA, A., BUTU, M., Mat. Plast., **45**, no. 4, 2008, p. 351
22. CURTU, I., MOTOC, D.L., Mat.Plast., **45**, no. 4, 2008, p. 366
23 TABACU, ŞT., HADĂR, A., MARINESCU, D., IVĂNESCU, M., BĂLĂŞOIU, V., Mat. Plast., **46**, no. 2, 2009, p. 192
24. ILIESCU, N., HADĂR, A., PASTRAMĂ, ŞT.,D., Mat. Plast., **46**, no. 1, 2009, p. 91
25. TABACU, ŞT., HADĂR, A., MARIN, D., DINU, G., IONESCU, D.S., Mat. Plast., **45**, no. 1, 2008, p. 113
26. ILIESCU, N., ATANASIU, C., HADĂR, A., Mat. Plast., **42**, no. 1, 2005, p. 72
27. HADĂR, A., CONSTANTINESCU, I.N., JIGA, G., IONESCU, D.S., Mat. Plast, **44**, no. 4, 2007, p. 354
28. HADĂR, A., BORDEAŞU, I., MITELEA, I., VLASCEANU, D., Mat. Plast., **43**, no. 1, 2006, p. 70
29. POPESCU, D., HADĂR, A., COTEŢ, C., Mat. Plast, **43**, no. 2, 2006, p. 175
30. SPÂNU, A., HADĂR, A., DRĂGOI, G., Mat. Plast., **43**, no. 3, 2006, p. 199

Manuscript received: 11.12.2009